ORIGINAL ARTICLE

Tuning the hydrophilic–hydrophobic balance of block-graft copolymers by click strategy: synthesis and characterization of amphiphilic PCL-*b*-(PαN₃CL-*g*-PBA) copolymers

Ren-Shen Lee and Yi-Ting Huang

The self-organization of amphiphilic block copolymers in water strongly depends on their molecular structure, particularly their hydrophilic–hydrophobic balance. This study proposes tuning the amphiphilicity of block copolymers by a click strategy. This work prepares novel amphiphilic block-graft PCL-*b*-(PαN₃CL-*g*-PBA) copolymers that comprise poly(ε-caprolactone) (PCL) as the hydrophobic segment and poly(α-azido-ε-caprolactone-graft-propargyl benzoate) (PαN₃CL-*g*-PBA) as the hydrophilic segment by ring-opening polymerization of 2-chloro-ε-caprolactone (ClCL) with hydroxyl-terminated macroinitiator PCL, substituting pendent chloride with sodium azide. This copolymer is subsequently used for grafting propargyl benzoate (PBA) moieties by the Cu(I)-catalyzed Huisgen's 1,3-dipolar cycloaddition, thus producing a 'click' reaction. This research examines characteristics of these copolymers by ^{1}H NMR, FT-IR, GPC, contact angle measurement and differential scanning calorimetry (DSC). Increasing the length of the hydrophilic segment or decreasing the length of the hydrophobic segment significantly increases water uptake and decreases the contact angle of the copolymers. These amphiphilic copolymers self-assembled into micelles in the aqueous phase, which were then examined by fluorescence, dynamic light scattering (DLS) and transmission electron microscopy (TEM). The average micelle size ranges from 90 to 190 nm. The critical micelle concentration (CMC) is from 2.4 to 7.6 mg l^{-1} at 25 °C. The length of the hydrophilic segment influences the shape of the micelle. The current study describes drug entrapment efficiency and drug loading content of micelles, dependent on the composition of block-graft polymers.
Polymer Journal (2010) **42**, 304–312; doi:10.1038/pj.2010.6; published online 24 February 2010

Keywords: amphiphilic; block-graft copolymers; click chemistry; hydrophilic–hydrophobic balance; micelles

INTRODUCTION

Amphiphilic copolymers are well known for self-assembly into micelles or larger aggregates in solvents selective to one block. In aqueous solutions, a core-shell structure commonly forms with a hydrophobic core surrounded by a hydrated hydrophilic shell. Previous researches have extensively studied[1–5] the properties of block copolymer micelles in biomedical applications, namely the efficacious delivery of hydrophobic drugs sequestered within micellar cores.

The parameter which principally governs self-organization of amphiphilic block copolymers is hydrophilic–hydrophobic balance, even though other experimental factors such as concentration, pH, ionic strength, temperature and sample preparation may also influence aggregation mechanisms.[6] Hence, the macromolecular structure of block copolymer aggregates somewhat predetermines their nanoscale morphology.[7,8] Modifying the hydrophilic–hydrophobic balance of diblock copolymers via coupling with additional hydrophilic or hydrophobic moieties is a possibility.[9,10]

The copper-catalyzed 1,3-dipolar cycloaddition of azides and terminal alkynes is potentially a very interesting reaction for modifying block copolymer aggregates.[11,12] This particular reaction is very efficient, highly selective and generally proceeds very high yield in either organic or aqueous media, requiring only mild experimental conditions.[13] Thus, this versatile reaction has lately been described as the archetype of 'click' chemistry.[14] Owing to the simplicity and selectivity of these reactions, recent research works have extensively studied copper-catalyzed azide-alkyne cycloadditions in biological and material science.[15–22]

This work investigates copper-catalyzed azide-alkyne cycloadditions as a tool for varying the hydrophilic–hydrophobic balance of diblock copolymers in aqueous medium. This approach clicks a model AB amphiphilic block copolymer composed of a poly(ε-caprolactone) (PCL) hydrophobic segment and a poly(α-azo-ε-caprolactone-graft-propargyl benzoate) (PαN₃CL-*g*-PBA) hydrophilic segment with additional hydrophilic alkyne (Scheme 1). This work studies
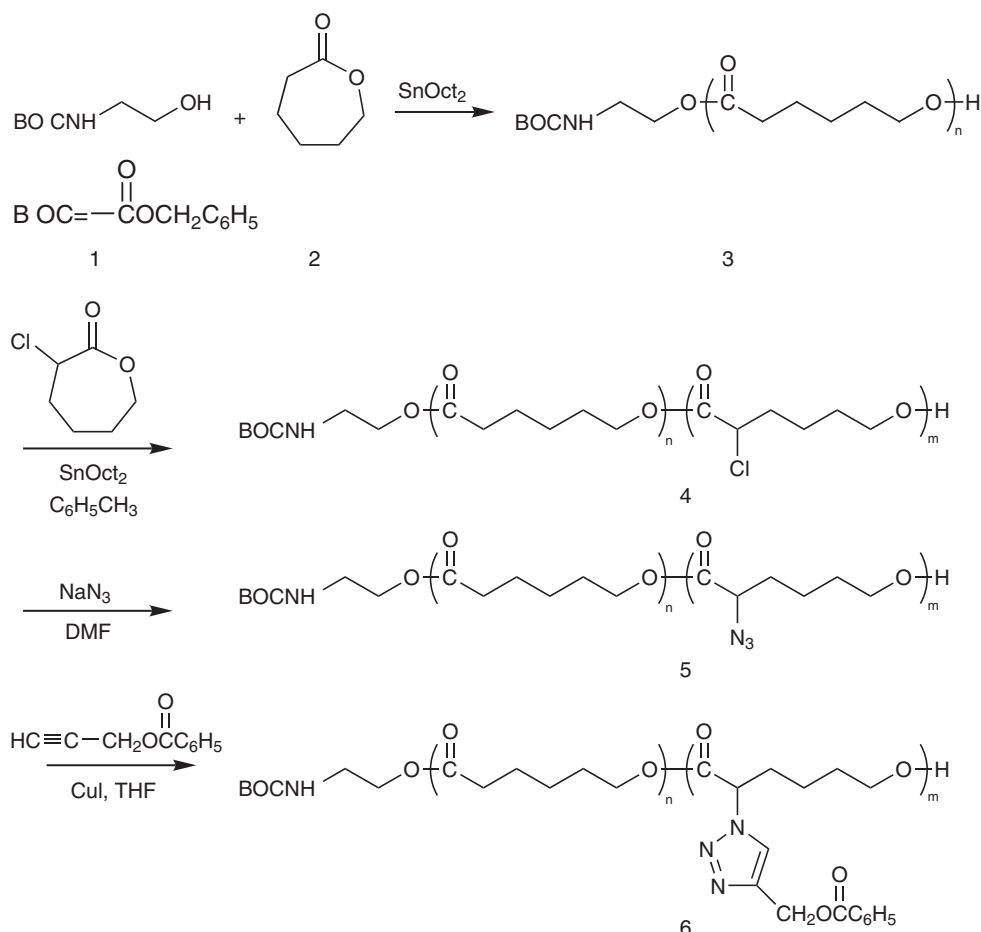
Scheme 1 Strategy for the synthesis of block-graft PCL-b-(PαN₃CL-g-PBA).

the influence of hydrophilic/hydrophobic chain length of block copolymer on micelle size, drug entrapment efficiency and drug loading content. The micellar characteristics of these block-graft copolymers in an aqueous phase were investigated with fluorescence spectroscopy, dynamic light scattering and transmission electron microscopy.

EXPERIMENTAL PROCEDURE

Materials
Benzyl N-(2-hydroxyethyl)carbamate, 2-chlorocyclohexanone, pyrene, propargyl benzoate, amitriptyline hydrochloride (AM), and sodium azide were purchased from Aldrich Chemical Co. (Milwaukee, WI, USA). m-Chloroperoxybenzoic acid was purchased from Fluka Chemical Co. (Buchs SG1, Switzerland). Stannous octoate (SnOct₂) was purchased from Strem Chemical Co. (Newburyport, MA, USA). ε-CL was dried and vacuum-distilled over calcium hydride. αClCL was prepared according to a reported method.[23] Organic solvents such as tetrahydrofuran (THF), methanol, chloroform, toluene, N,N-dimethylformamide (DMF) and n-hexane were a high-pressure liquid chromatography grade and were purchased from Merck Chemical (Darmstadt, Germany). Ultrapure water was obtained by purification with a Milli-Q Plus (Waters, Milford, MA, USA).

Preparation of PCL macroinitiators
Hydroxyl-terminated functional PCL was prepared with benzyl N-(2-hydroxyethyl)carbamate initiating the ring-opening polymerization of ε-CL. A total of 0.765 mmol of benzyl N-(2-hydroxyethyl)carbamate and 7.65 mmol of ε-CL was polymerized in the melt at 110 °C for 8 h. The crude polymers were dissolved in CHCl₃, microfiltered, and then precipitated into excess CH₃OH

with stirring. After purification, the PCL macroinitiators were dried in vacuo at 50 °C for 24 h. Figure 1a shows the representative ¹H NMR spectrum of PCL29.

Synthesis of PCL-b-PαClCL diblock copolymers
All glasses were dried in the oven and handled under a dry nitrogen stream. The typical polymerization process to give PCL29-b-PαClCL31 is as follows. PCL29 (M_n=4350 g mol⁻¹; 0.73 g, 0.17 mmol) and αClCL (0.75 g, 5.03 mmol) were added to a flask and heated under a dry nitrogen stream to dissolve PCL29. Next, 22 mg of SnOct₂ (1.5 wt% based on the weight of PCL and αClCL) and toluene (30 ml) were added to the flask. The flask was purged with nitrogen and the reaction solution was refluxed for 48 h. The solution was concentrated with a vacuum rotary evaporator. The resulting product was dissolved in CHCl₃ and then precipitated into excess n-hexane/ethyl ether (v/v 5:1) with stirring. The purified polymer was dried in vacuo at 50 °C for 24 h and then analyzed. The yields ranged between 72 and 83%. Figures 1b and 2a show the representative ¹H NMR and IR spectra of PCL29-b-PαClCL31.

Synthesis of PCL-b-PαN₃CL diblock copolymers
PCL29-b-PαClCL31 (1.78 g, 0.22 mmol, 31 equiv of αClCL) was dissolved in 10 ml of DMF in a glass reactor followed by the addition of NaN₃ (10.9 mmol). The mixture was stirred overnight at room temperature. The insoluble salt was removed by filtration and elimination of DMF in vacuo. The resulting product was dissolved in CHCl₃ and then precipitated into excess n-hexane/ethyl ether (v/v 4:1) with stirring. The purified polymer was dried in vacuo at 50 °C for 24 h and then analyzed. The yields ranged between 75 and 84%. Figures 1c and 2b show the representative ¹H NMR and IR spectra of PCL29-b-PαN₃CL28.
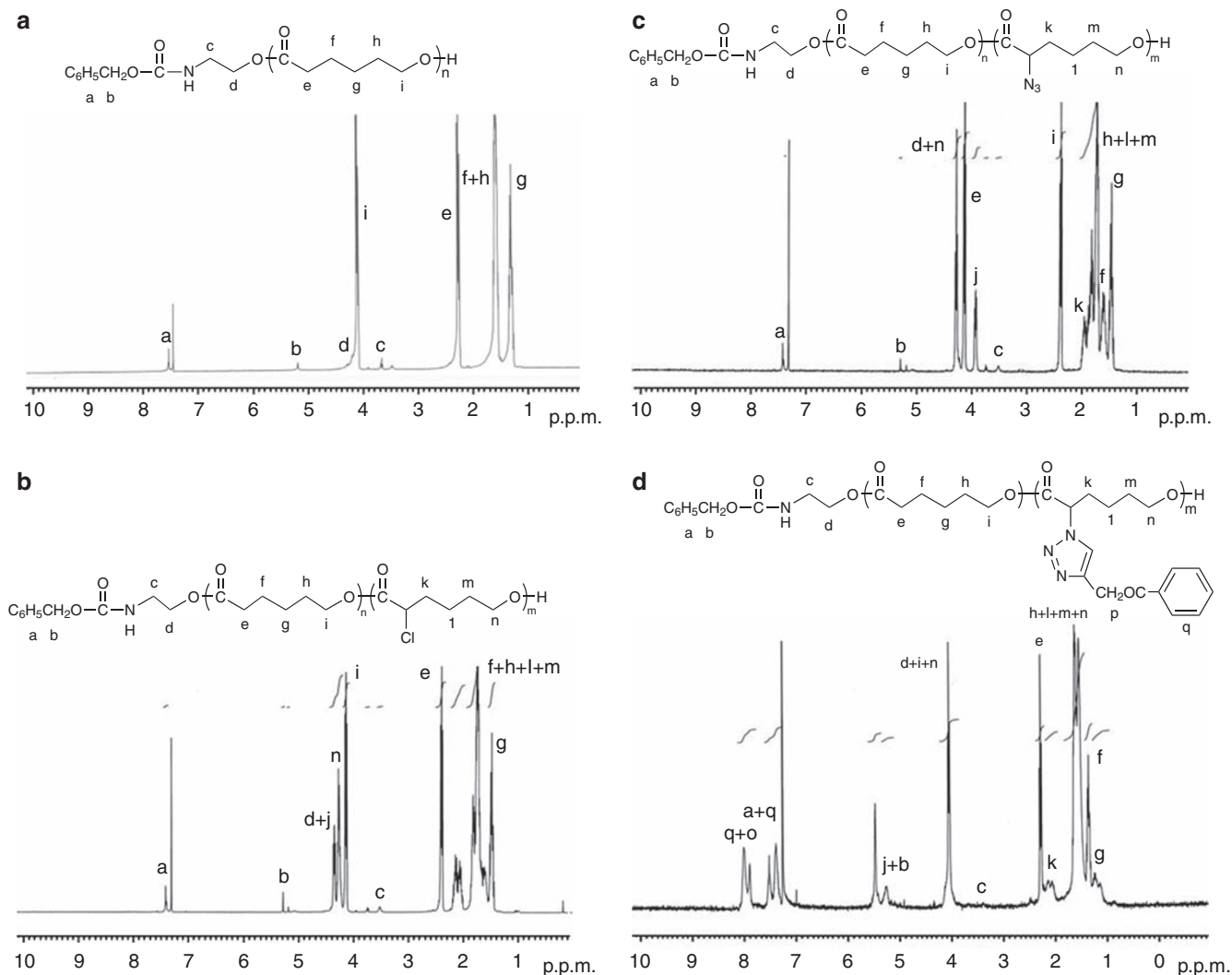
Figure 1 Representative ¹H NMR spectroscopy of (**a**) PCL29, (**b**) PCL29-*b*-PαClCL31, (**c**) PCL29-*b*-PαN₃CL28, (**d**) PCL29-*b*-(PαN₃CL28-*g*-PBA21).

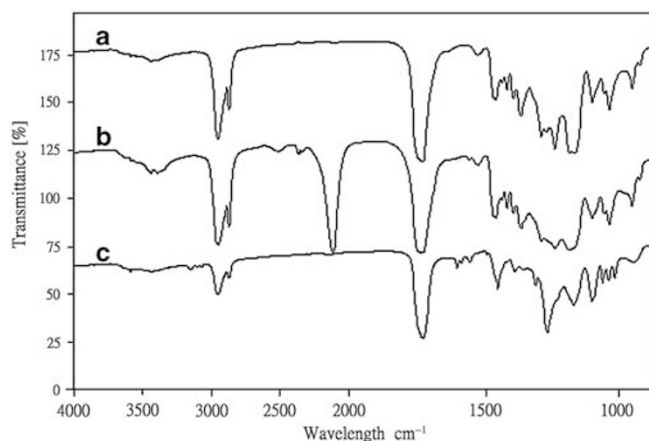**Figure 2** IR spectra of (a) PCL29-*b*-PαClCL31, (b) PCL29-*b*-PαN₃CL28, (c) PCL29-*b*-(PαN₃CL28-*g*-PBA21).

Typical click chemistry reaction

PCL29-*b*-PαN₃CL28 (27.9 mmol, 0.78 mol equiv of azide) was transferred into a glass reactor containing THF. Propargyl benzoate (0.94 mol), CuI (9.4 mmol),

and triethyl amine (9.4 mmol) were then added to the reactor. The solution was stirred at 35 °C for 4 h. The cycloaddition copolymer was precipitated in hexane with stirring. The purified polymer was dried *in vacuo* at 50 °C for 24 h and then analyzed. Figures 1d and 2c show the representative ¹H NMR and IR spectra of PCL29-*b*-(PαN₃CL28-*g*-PBA21).

Characterization

¹H NMR spectra were recorded at 500 MHz (with a Bruker WB/DMX-500 spectrometer, Ettlingen, Germany) with chloroform (δ=7.24 p.p.m.) as an internal standard in chloroform-*d* (CDCl₃). A thermal analysis of the polymer was performed on a DuPont 9900 system that consisted of DSC (Newcastle, DE, USA). The heating rate was 20 °C min⁻¹. Glass-transition temperatures (T_gs) were read at the middle of heat capacity change and taken from the second heating scan after quick cooling. Number- and weight-average molecular weights (M_n and M_w, respectively) of the polymer were determined by a GPC system, carried out on a Jasco high-pressure liquid chromatography system equipped with a model PU-2031 refractive-index detector (Tokyo, Japan) and Jordi Gel DVB columns with pore sizes of 100, 500 and 1000 Å. Chloroform was used as an eluent at a flow rate of 0.5 ml min⁻¹. PEG standards with a low dispersity (Polymer Sciences, Mainz, Germany) were used to generate a calibration curve. Data were recorded and manipulated with a Windows-based software package (Scientific Information Service, Augustine, Trinidad & Tobago). UV-vis spectra were obtained using a Jasco V-550

spectrophotometer (Tokyo, Japan). The pyrene fluorescence spectra were recorded on a Hitachi F-4500 spectrofluorometer (Japan). Square quartz cells of 1.0×1.0 cm were used. For fluorescence excitation spectra, the detection wavelength (λem) was set at 390 nm. The water contact angle of polymer films were measured statically on a FTA-1000 contact angle meter (First Ten Ångstroms, Portsmouth, VA, USA) using deionized water as the probe liquid. Water sorption was evaluated by immersing polymer films in distilled water for 24 h at 37 °C and then weighing them at regular intervals for 3 h until constant weight. Water sorption was calculated as follows:

$$\text{Water sorption}\,(\%) = \{[W_{\text{wet}} - W_{\text{dry}}]/W_{\text{dry}}\} \times 100$$

where W_{wet} is the weight of the polymer film immediately after being removed from the water and having the surface water removed by filter paper, and W_{dry} is the weight of the wet film after rigorous drying in vacuum at 50 °C until constant weight.

Preparation of polymeric micelles
Polymeric micelles of PCL-b-(PαN₃CL-g-PBA) copolymers were prepared using the oil-in-water (o/w) emulsion technique. Briefly, 30 mg of each polymer was dissolved in dichloromethane (MC, 5 ml). The solution was added dropwise into DI water (100 ml) with vigorous stirring at ambient temperature. Next, the emulsion solution was ultrasonicated for 1 h and stirred overnight at ambient temperature. After the MC completely evaporated, the experiment yielded a polymeric micelle solution.

Measurements of the fluorescence spectroscopy
To confirm micelle formation, fluorescence measurements were carried out using pyrene as a probe.[24] Fluorescence spectra of pyrene in aqueous solution were recorded at room temperature on a fluorescence spectrophotometer. The sample solutions were prepared by first adding known amounts of pyrene in acetone to a series of flasks. After the acetone had evaporated completely, measured amounts of micelle solutions with various concentrations of PCL-b-(PαN₃CL-g-PBA) ranging from 2.93 to 150 mg l⁻¹ were added to each flask and mixed by vortexing. The pyrene concentration in the final solutions was 6.1×10^{-7} M. The flasks were allowed to stand overnight at room temperature to equilibrate the pyrene and the micelles. The emission wavelength was 390 nm for excitation spectra.

Measurements of the size and size distribution
Size distributions of the micelles were estimated by dynamic light scattering using a particle-size analyzer (Zetasizer nano ZS, Malvern, UK) at 20 °C. Scattered light intensity was detected at 90° to an incident beam. Measurements were made after the aqueous micellar solution ($C = 2.93–300$ mg l⁻¹) was passed through a microfilter with an average pore size of 0.2 μm (Advantec MFS, Dublin, CA, USA). An average size distribution of aqueous micellar solution was determined based on CONTIN programs of Provencher and Hendrix.[25]

Transmission electron microscopy observations
The morphology of the micelles was observed by transmission electron microscopy (JEM 1200-EXII, Tokyo, Japan). Drops of micelle solution ($C = 0.3$ g l⁻¹, no containing stain agent) were placed on a carbon film coated on a copper grid, and were then dried at room temperature. The observation was conducted at an accelerating voltage of 100 kV.

Determination of drug-loading content and drug entrapment efficiency
Using oil-in-water solvent evaporation, PCL-b-(PαN₃CL-g-PBA) (10 mg) was dissolved in 6 ml methylene chloride followed by adding AM, serving as a model drug at various weight ratios to the polymer (1/10–1/1). The solution was added dropwise to 150 ml of distilled water containing 1 wt% poly(vinyl alcohol) under vigorous stirring. Poly(vinyl alcohol) was used as a surfactant to reduce micelle aggregation. Sonication at ambient temperature for 60 min reduced the droplet size. The emulsion was stirred overnight at ambient temperature to evaporate the methylene chloride. The aggregated AM-loaded micelles were removed by centrifugation (3000 r.p.m.×30 min). Next, the aqueous micellar solution was dried at room temperature by a vacuum rotary evaporator. The unloaded AM was eliminated by washing three times with distilled water because AM solubility in water is much larger than that of the block copolymer and the micelles. The micelles were obtained by vacuum drying. A weighed amount of micelles was disrupted by adding acetonitrile (10 ml). Drug content was assayed spectrophotometrically at 240 nm using a diode array UV-vis spectrophotometer. The drug-loading content and drug entrapment efficiency were calculated by equations (1) and (2), respectively:

$$\text{Drug-loading content}\,(\%) = (\text{weight of drug in micelles/weight of micelles}) \times 100 \quad (1)$$

$$\text{Drug entrapment efficiency}\,(\%) = (\text{weight of drug in micelles/weight of drug fed initially}) \times 100 \quad (2)$$

In vitro degradation
In vitro degradation of about 30 mg of copolymer thin film was performed in 5 ml PBS (0.067 M, pH 7.4) at 37 °C, and the buffer solution was replaced every 2 days. At specific time intervals, the specimen was removed, washed with distilled water, lyophilized and weighed. Weight loss $(\%) = 100(D_0 - D)/D_0$ where D_0 is the copolymer weight before degradation and D is the copolymer weight after degradation for a certain period.

RESULTS AND DISCUSSION
Synthesis of the PCL-b-PαClCL diblock copolymers
Various PCL-b-PαClCL diblock copolymers were obtained via the ring-opening polymerization of αClCL with hydroxyl-terminated macroinitiator PCL. Scheme 1 illustrates the synthesis of PCL-b-PαClCL diblock copolymers. First, the hydroxyl-terminated PCL was prepared by ring-opening homopolymerization of ε-CL with initiator benzyl N-(2-hydroxyethyl)carbamate (at molar ratios 30/1, 60/1 and 80/1) in the presence of SnOct₂ in bulk at 110 °C for 8 h.[26] Table 1

Table 1 Result of macroinitiator prepared by ring-opening polymerization of ε-CL with initiator benzyl N-(2-hydroxyethyl)carbamate in bulk at 110 °C with 1.5 wt% SnOct₂ as the catalyst for 8 h

Macroinitiator	[ε-CL]/[I] molar ratio in the feed	[ε-CL]/[I] molar ratio[a]	$M_{n,th}$[b]	$M_{n,GPC}$[c]	M_w/M_n[c]	$M_{n,NMR}$[d]
PCL29	30/1	29/1	3620	4350	1.57	3500
PCL60	60/1	60/1	7040	6990	1.55	7040
PCL96	80/1	96/1	9320	8680	1.69	11 140

[a]Determine by ¹H NMR spectroscopy.
[b]$M_{n,th}$ $M_{\text{initiator}} + M_{\varepsilon-CL} \times [M]/[I]$ ($M_{\text{initiator}}$ is the molecular weight of initiator, $M_{\varepsilon-CL}$ is the molecular weight of ε-CL, [M] is the monomer molarity concentration, and [I] is the initiator molarity concentration).
[c]Determined by GPC.
[d]Determined by ¹H NMR spectroscopy of PCL.

Table 2 Result of the block copolymerization of 2-chloro-ε-caprolactone (αClCL) initiated with hydroxyl-terminated PCL and substitution of PCL-*b*-PαClCL by sodium azide

Copolymer	[αCl(N₃)CL]/[PCL] molar ratio in the feed	[αCl(N₃)CL]/[PCL] molar ratio[a]	Yeild (%)	$M_{n,th}$[b]	$M_{n,NMR}$[a]	$M_{n,GPC}$[c]	M_w/M_n[c]	T_g (°C)[d]	T_m (°C)[d]	ΔH_f (J/g)[d]
PCL-b-PαClCL										
PCL29-*b*-PαClCL14	10/1	14/1	72	4990	5580	5110	1.71	−49	49	41
PCL29-*b*-PαClCL31	30/1	31/1	83	7960	8110	7540	1.61	−49	45	30
PCL60-*b*-PαClCL34	30/1	34/1	76	11490	12080	11900	1.14	−47	53	41
PCL96-*b*-PαClCL34	30/1	34/1	79	15600	16190	12860	1.44	−46	53	44
PCL-b-PαN₃CL										
PCL29-*b*-PαN₃CL6	14/1	6/1	76	5670	4430	5000	1.74	−47	49	29
PCL29-*b*-PαN₃CL28	31/1	28/1	84	8310	7840	8210	1.57	−47	47	25
PCL60-*b*-PαN₃CL34	34/1	34/1	75	12310	12310	12970	1.17	−46	51	34
PCL96-*b*-PαN₃CL28	34/1	28/1	80	16410	15480	12840	1.69	−46	52	35

[a]Determined by ¹H NMR spectroscopy.
[b]$M_{n,th}M_{n,NMR}$ of PCL+$M_{\alpha ClCL}$ (or $M_{\alpha N3CL}$)×[M]/[I] (where $M_{\alpha ClCL}$ is the molecular weight of αClCL, $M_{\alpha N3CL}$ is the molecular weight of αN₃CL. [M] is the monomer molarity concentration, and [I] is the initiator molarity concentration).
[c]Determined by GPC.
[d]Determined from DSC thermograms.

compiles the results of the polymerization. The number-average molecular weight (M_n) of the macroinitiators are in agreement with $M_{n,th}$ and $M_{n,NMR}$ except for the PCL80. This is because the hydroxyl-terminal group of PCL is more reactive than that of *N*-(2-hydroxyethyl)carbamate. The length of PCL in PCL96 exceeded the expected value. The polydispersities are also narrow for bulk polymerizations. Figure 1a shows the typical ¹H NMR spectrum of the PCL29.

This study used the hydroxyl group of the macroinitiator as the initiation site for the ring-opening polymerization of αClCL in the presence of SnOct₂ (1.5 wt%) as the catalyst at reflux with toluene for 48 h. Table 2 compiles the results of the polymerization. The yields were high, ranging between 72 and 83%. The M_n of block copolymers obtained from copolymerization of the αClCL and PCL macroinitiator increased with the increase of the molar ratio of the αClCL to PCL macroinitiator in the feed. The number-average molecular weight (M_n) of the block copolymers were in agreement with $M_{n,th}$. When using PCL29 as the macroinitiator, the molar ratio of αClCL to PCL29 in the feed increased from 10 to 30, and the M_n of the copolymers increased from 5110 to 7540 g mol⁻¹ with M_w/M_n between 1.61 and 1.71. When using PCL 60 or PCL96 as the macroinitiator, the molar ratios of αClCL to PCL in the feed were fixed at 30, and the obtained M_n values of the copolymers were 11900, and 12860 g mol⁻¹, respectively. The molar compositions of the block copolymers were analyzed by ¹H NMR. The amounts of comonomer incorporated into the copolymer were calculated from comparing the integral area of the resonance peak δ=2.30–2.41 p.p.m. of the second carbon (C₂) methylene protons of PCL with the resonance peaks δ=1.91–2.09 p.p.m. of the third carbon (C₃) methylene protons of PαClCL. From the ¹H NMR analysis, copolymerization conversion of the monomers was slightly larger than that of the corresponding feeds. Figure 1b shows the typical ¹H NMR spectrum of the block copolymer PCL29-*b*-PαClCL31. The resonance peaks are assigned to the corresponding hydrogen atoms of the copolymers. Observations show typical signals of the PCL blocks at δ=1.42 (H_g, C₄ methylene protons), 1.51–1.89 (H_{f+h}, C₃ and C₅ methylene protons), 2.38 (H_e, C₂ methylene protons), and 4.08 p.p.m. (H_i, C₆ methylene protons). The resonance peaks of PαClCL blocks are seen at δ=1.51–1.89 (H_{l+m}, C₄ and C₅ methylene protons), 1.95–2.18 (H_k, C₃ methylene protons), 4.21 (H_n, C₆ methylene protons), and 4.29 p.p.m. (H_j, C₂ methine proton).

Substitution of the pendent Cl atoms of PCL-*b*-PαClCL by sodium azide

According to Scheme 1, the pendent chlorides of PCL-*b*-PαClCL must be converted into azides by reaction with sodium azide. PCL-*b*-PαClCL was thus reacted with 1 equiv of sodium azide in DMF overnight at room temperature. Table 1 compiles the substitution results. As expected, the IR spectrum shows a new absorption peak at 2106 cm⁻¹, which is characteristic of the azide (Figure 2b). ¹H NMR confirms that the conversion of the pendent chlorides into azides is almost quantitative. Indeed, the resonance peak at 4.29 p.p.m. for the C*H*Cl protons completely disappears to be replaced by a new peak at 3.88 p.p.m., typical of the C*H*N₃ protons (Figure 1c, peak j). The molar ratio [αN₃CL]/[PCL] in the block copolymers was analyzed by ¹H NMR and calculated by integrating the resonance peaks at δ=3.88 p.p.m. of the C*H*N₃ protons of PαN₃CL with the resonance peaks δ=7.39 p.p.m. of the initiator phenyl protons. Table 2 shows that the molecular weight of the copolymers is similar to that of the chloride substituent polymer. This observation is consistent with a small change in the hydrodynamic volume of the copolymer. The elution peak remains symmetrical and a slight increase in polydispersity is reported, strongly suggesting a lack of chain degradation (Figure 3). Figure 1c shows a typical ¹H NMR spectrum of the block copolymer PCL29-*b*-PαN₃CL28. The resonance peaks are assigned to the corresponding hydrogen atoms of the copolymers.

Thermal properties of PCL-*b*-PαClCL and PCL-*b*-PαN₃CL block copolymers

Table 2 shows the thermal behaviors of the block copolymers. The DSC observations show only a slight effect on the thermal transitions with increased incorporated amounts of αClCL (or αN₃CL). The chlorinated polyester (PαClCL) and PαN₃CL are amorphous with T_g at −44 and −43 °C, respectively.[27] Notably, PCL blocks can crystallize in PCL-*b*-PαClCL and PCL-*b*-PαN₃CL. The copolymers of PCL-*b*-PαClCL and PCL-*b*-PαN₃CL were semicrystalline, showing a T_m lower than that of the corresponding PCL (T_m=57 °C).[23] When the length of the PCL block was fixed and the length of the PαClCL (or PαN₃CL) block was increased, downward trends in T_m and in heat of fusion (ΔH_f) were observed. Based on the principle of polymer physics, the

polymer with lower crystallinity would have lower melting point and lower heat of fusion. Thus, the crystallinity of PCL would decrease with increasing incorporated content of PαClCL (or PαN₃CL).

However, fixing the length of the PαClCL (or PαN₃CL) block and increasing the length of PCL block produced no significant change in T_m. Similarly, this study showed no significant effect on T_g values with increasing amounts of αClCL (or αN₃CL) on copolymers PCL-*b*-PαClCL and PCL-*b*-PαN₃CL. The T_g of PCL-*b*-PαClCL and PCL-*b*-PαN₃CL were higher than that of PCL ($T_g=-61\,°C$). This is due to the steric hindrance and static effect of αClCL containing chloro-substituents (or αN₃CL containing azo-substituents) that reduce backbone flexibility.

Click reaction of PCL-*b*-PαN₃CL with alkyne

To functionalize the aliphatic polyesters, chemical transformation by click reaction between alkynes and azides is very appealing because of
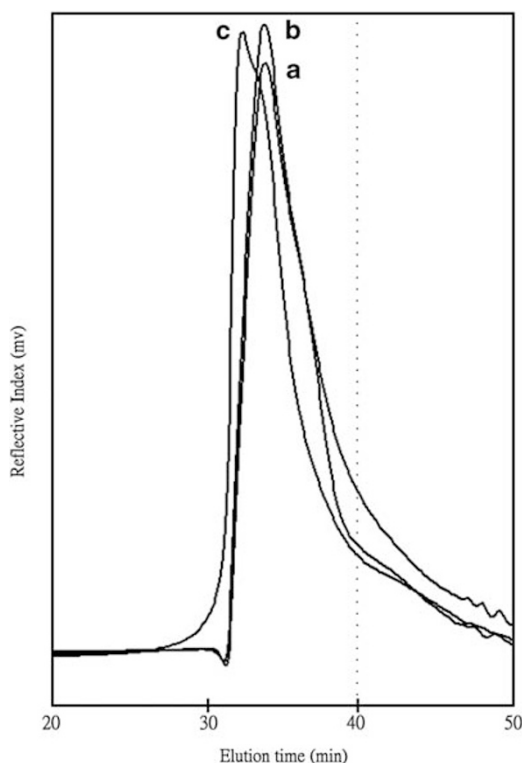

Figure 3 GPC curves of (a) PCL29-*b*-PαClCL31, (b) PCL29-*b*-PαN₃CL28, (c) PCL29-*b*-(PαN₃CL28-*g*-PBA21).

the mild conditions and quantitative yields. The click reaction was catalyzed by copper iodide and Et₃N in THF at a low temperature (35 °C) for 4 h. Table 3 compiles the cycloaddition results. The assumed molecular weight (theoretical number-average molecular weight ($M_{n,th}$)) was in good agreement with the GPC-determined number-average molecular weight ($M_{n,GPC}$) except for PCL96-*b*-(PαN₃CL28-*g*-PBA20). For PCL96-*b*-(PαN₃CL28-*g*-PBA20), the GPC-derived molecular weight (7110 g mol⁻¹) was much lower than $M_{n,th}$ (19 960 g mol⁻¹). This underestimation in molecular weight is most likely due to the impact of grafting density on hydrodynamic radius, giving these graft copolymers more compact structures than the linear standards used to calibrate the GPC.[28]

The grafting efficiency was only between 50 and 83%. This may be due to the steric hindrance of PCL-*b*-PαN₃CL and the catalyst copper(I) salt, which often show reduced selectivity.[17] Successful click reaction to yield a PBA-grafted polyester was confirmed by the disappearance of the azide signal at 2103 cm⁻¹ and a new absorption peak at 1608 cm⁻¹ characteristic of the vibration of the triazole unsaturated group observed in the FT-IR spectrum. Figure 3 shows the typical GPC curves of PCL29-*b*-(PαN₃CL28-*g*-PBA21) compared with those of the original PCL29-*b*-PαN₃CL28. The GPC traces show a unimodal distribution of the block copolymer and a peak shift toward a higher molecular weight region compared with the peak of the original PCL-*b*-PαN₃CL. According to ¹H NMR analysis, the cycloaddition confirmed that the peak for CHN₃ proton at 3.85 p.p.m. disappeared, and that a new peak for the triazole proton appeared at 7.95 p.p.m., indicating triazole formation. The extent of PBA incorporated into the copolymer was calculated by integrating ¹H NMR spectral signals at $\delta=5.48$ (I_p) against the signal at $\delta=2.29$ (I_e). As Table 3 shows, the spectroscopically calculated incorporations of PBA are similar to the feed ratios. However, some remaining PCL-*b*-(PαN₃CL) was observed in the ¹H NMR spectrum for some grafting reactions.

The block-graft PCL-*b*-(PαN₃CL-*g*-PBA) copolymers are semicrys-talline, with T_m in the range of 49–52 °C and T_g in the range of −48 to −43 °C. Observations show upward trends in T_m, ΔH_f and T_g of the copolymer with longer hydrophobic or hydrophilic segments. However, the heat of fusion for PCL29-*b*-(PαN₃CL28-*g*-PBA21), and PCL60-*b*-(PαN₃CL34-*g*-PBA17) were not found. This is due to the crystalline area of PCL having been destroyed by the incorporated PαN₃CL-*g*-PBA.

Micelles of block-graft copolymers

The amphiphilic nature of the block-graft copolymers, consisting of hydrophobic PCL and hydrophilic PαN₃CL-*g*-PBA block provides an opportunity to form micelles in water. The characteristics of the block-graft copolymer micelles in an aqueous phase were investigated

Table 3 Result of the grafting of PCL-*b*-PαN₃CL with 2-propargyl benzoate (PBA) by click reaction

Graft copolymer	[PBA]/[PCL-b-PαN₃CL] molar ratio in the feed	[PBA]/[PCL-b-PαN₃CL] molar ratio[a]	Grafting efficiency (%)	$M_{n,th}$[b]	$M_{n,NMR}$[a]	$M_{n,GPC}$[c]	M_w/M_n[c]	T_g (°C)[d]	T_m (°C)[d]	ΔH_f (J/g)[d]
PCL29-*b*-(PαN₃CL6-*g*-PBA5)	6/1	5/1	83	5390	5230	5590	1.57	−48	49	27
PCL29-*b*-(PαN₃CL28-*g*-PBA21)	28/1	21/1	75	12320	11200	10410	1.50	−46	50	—
PCL60-*b*-(PαN₃CL34-*g*-PBA17)	34/1	17/1	50	17750	15030	13480	1.39	−45	50	—
PCL96-*b*-(PαN₃CL28-*g*-PBA20)	28/1	20/1	71	19960	18680	7110	1.47	−43	52	31

[a]Determined by ¹H NMR spectroscopy of PCL-*b*-(PαN₃CL-*g*-PBA).
[b]$M_{n,th}$, $M_{n,NMR}$ of PCL-*b*-PαN₃CL+M_{PBA}×[PBA]/[PCL-*b*-PαN₃CL], (where M_{PBA} is the molecular weight of PBA, [PBA] is the PBA molarity concentration, and [PCL-*b*-PαN₃CL] is the polymer PCL-*b*-PαN₃CL molarity concentration).
[c]Determined by GPC.
[d]Determined from DSC thermograms.

by fluorescence techniques. The critical micelle concentrations of the block-graft copolymers in an aqueous phase were determined by a fluorescence technique using pyrene as a probe.
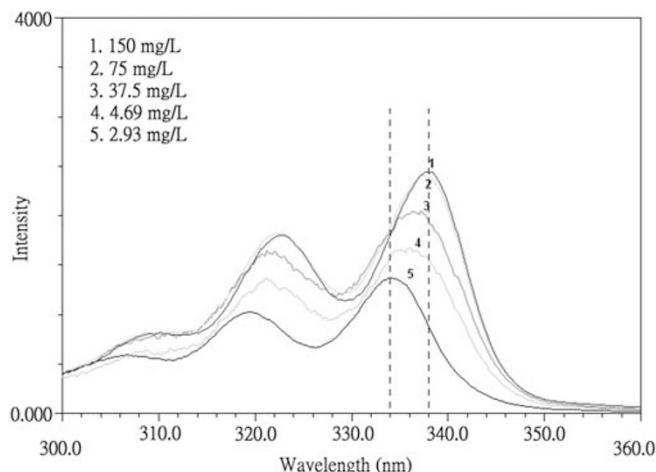

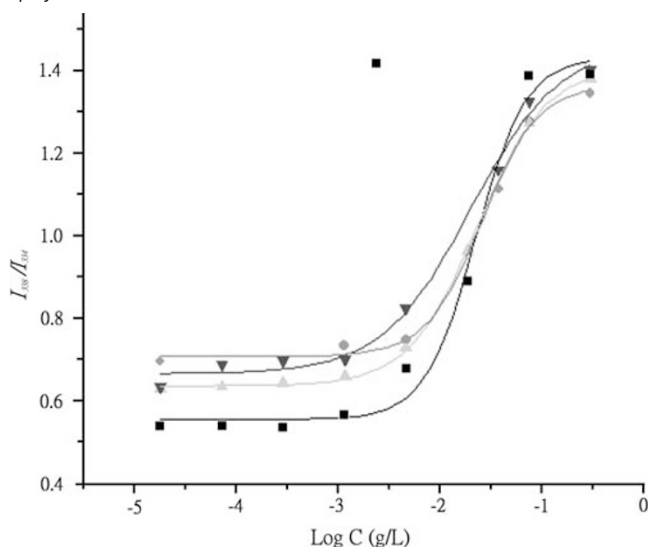**Figure 4** Excitation spectra of the PCL60-*b*-(PαN₃CL34-*g*-PBA17) copolymer monitored at λem=390 nm.

Figure 5 Plot of I_{338}/I_{334} intensity ratio (from pyrene excitation spectra; pyrene concentration=6.1×10^{-7} M) versus the logarithm of concentration (log C) for (■) PCL29-*b*-(PαN₃CL28-*g*-PBA21), (▲) PCL29-*b*-(PαN₃CL6-*g*-PBA5), (▼) PCL96-*b*-(PαN₃CL28-*g*-PBA20), (□) PCL60-*b*-(PαN₃CL34-*g*-PBA17).

Figure 4 shows the excitation spectra of pyrene in the PCL60-*b*-(PαN₃CL34-g-PBA17) solution at various concentrations. Findings show that fluorescence intensity increases with the increase in concentration of PCL60-*b*-(PαN₃CL34-g-PBA17). The characteristic feature of pyrene excitation spectra, a red shift of the (0,0) band from 334 to 338 nm upon pyrene partition into micellar hydrophobic core, was used to determine the CMC values of PCL-*b*-(PαN₃CL-g-PBA) block-graft copolymers. Figure 5 shows the intensity ratios (I_{338}/I_{334}) of pyrene excitation spectra versus the logarithm of concentration of PCL-*b*-(PαN₃CL-g-PBA) block-graft copolymers. The CMC was determined from intersecting straight-line segments drawn through the points at the lowest polymer concentrations, which lay on a nearly horizontal line, passing through the points on the rapidly rising part of the plot. Table 4 shows CMC values of the block-graft copolymers dependent on block composition. The CMC of block-graft copolymers was in the range of 2.4–7.6 mg l⁻¹. The value is comparable to those of other polymeric micelles (for example, the CMC of MPEG-*b*-(PαN₃CL-g-alkyne) was 1.4–12 mg l⁻¹).[22] Generally, if the hydrophilic block is kept constant for a series of copolymers, an increase in the molecular weight of the hydrophobic block will decrease the CMC. To a lesser extent, if constant length of the hydrophobic block is maintained, then an increase in the length of the hydrophilic block will cause an increase in the value of the CMC.[29] In this study, the relationship between CMC and hydrophilicity was also consistent. At a fixed length of the hydrophobic block, the length of the hydrophilic segment increased and CMC values increased.

The mean hydrodynamic diameters of micelles without AM from dynamic light scattering were in the range of 90–190 nm. Fixing the concentration at 50-fold of the CMC value (50×CMC), the mean diameter of micelles increased with increasing ratio of the lengths of the hydrophobic segment to the hydrophilic segment. Figure 6 shows a similar trend in morphology of the micelles. The ratio of the hydrophobic segment to the hydrophilic segment also influences the shape of the micelle. As the length of hydrophobic segment increased, micelle morphology converted from a spherical to a spindle shape, presumably because of the strong repulsion of the hydrophobic blocks from the environment.[30] The effect of micelle concentration on the micelle size was also investigated (Table 5). As the concentration decreased from 300 to 2.93 mg l⁻¹, the sizes increased from 177 to 193 nm, and from 94 to 113 nm for PCL29-*b*-(PαN₃CL6-g-PBA5), and PCL29-*b*-(PαN₃CL28-g-PBA21), respectively. This is due to the hydration diameter increase in a dilute micelle solution.

Evaluation of drug-loading content and drug entrapment efficiency
This work calculated an amount of AM incorporated into block-graft PCL-*b*-(PαN₃CL-g-PBA) micelles by the ratio of the weight of AM in

Table 4 Properties of AM-loaded PCL-*b*-(PαN₃CL-*g*-PBA) grafted copolymer micelles

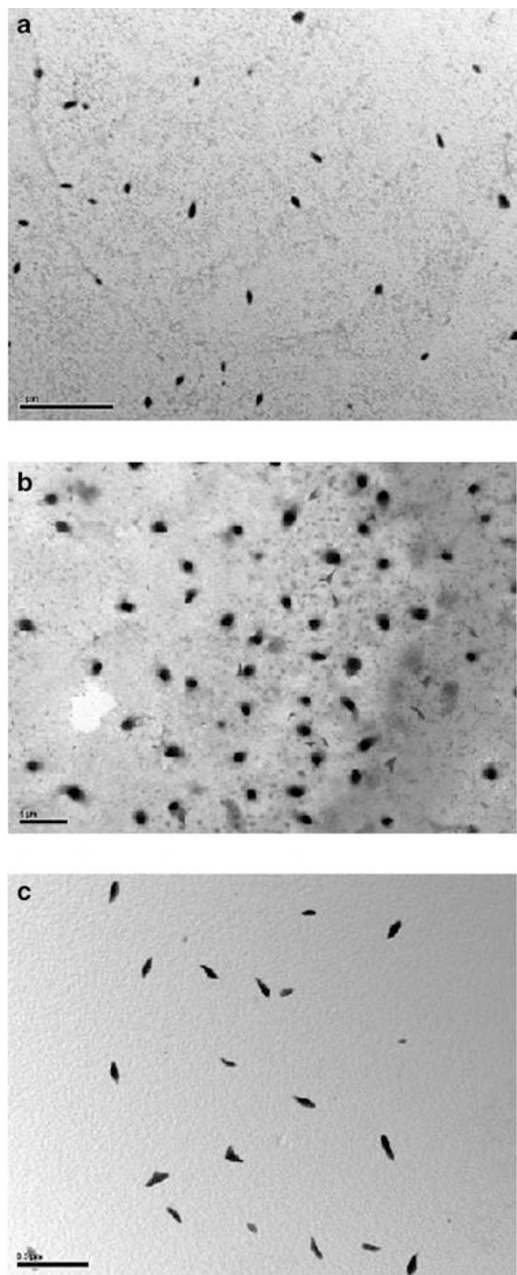| Copolymer	CMC (mg l⁻¹)	Feed weight ratio (AM/polymer)	Drug entrapment efficiency (%)	Drug-loading content (%)	Micelle size (nm)	
					Without AM	With AM
PCL29-*b*-(PαN₃CL28-*g*-PBA21)	7.6	1/10	9.6	1.5		
PCL29-*b*-(PαN₃CL28-*g*-PBA21)	7.6	1/5	10.0	1.7		
PCL29-*b*-(PαN₃CL28-*g*-PBA21)	7.6	1/2	16.4	4.1		
PCL29-*b*-(PαN₃CL28-*g*-PBA21)	7.6	1/1	21.8	10.9	87±6	403±125
PCL29-*b*-(PαN₃CL6-*g*-PBA5)	6.5	1/1	3.5	1.8	102±41	297±66
PCL60-*b*-(PαN₃CL34-*g*-PBA17)	2.9	1/1	28.5	13.3	109±45	219±37
PCL96-*b*-(PαN₃CL28-*g*-PBA20)	2.4	1/1	38.5	15.5	148±23	239±48

Figure 6 TEM photograghs of micelles formed by the (**a**) PCL29-*b*-(PαN₃CL28-*g*-PBA21), (**b**) PCL29-*b*-(PαN₃CL6-*g*-PBA5), (**c**) PCL96-*b*-(PαN₃CL28-*g*-PBA20) in THF/Water.

the nanosphere to the pre-weighted AM-loaded micelles, calculated by absorbance measurement after removing free AM and AM bounded on the micelle surface by sonication with distilled water. Table 4 shows the amount of AM introduced into the micelle by controlling the weight ratio between the drug and the polymer. Drug entrapment efficiency and drug loading content increased with the weight ratio of drug to polymer. In addition, drug entrapment efficiency and drug loading content were dependent on the polymer composition described. At a constant feed weight ratio (1/1), drug entrapment efficiency and drug loading content increased with increase in hydrophobic length. These results were attributed to the longer hydrophobic segment in the block copolymers, which enhance the drug amount entrapped in micelles. However, observations showed an inconsistent result in PCL29-*b*-(PαN₃CL6-g-PBA5). Furthermore, by comparing the sizes of loaded and unloaded AM drug micelles, the size increased when AM was loaded into the PCL-*b*-(PαN₃CL-g-PBA) micelles (Table 4).

Hydrophilicity of PCL-*b*-(PαN₃CL-g-PBA) copolymers
The surface and bulk hydrophilicities of various PCL-*b*-(PαN₃CL-g-PBA) copolymers with different feed ratios of components were determined by contact angles and water uptake, and the data are presented in Table 6. Observations showed increased water contact angles and reduced water uptake when the feed ratios of the hydrophobic block PCL were higher or when the feed ratios of the hydrophilic block PαN₃CL-g-PBA were lower. This means that introducing higher PCL or lower PαN₃CL-g-PBA segments lowers the surface hydrophilicity of the copolymers, resulting in a PαN₃CL-g-PBA that is more hydrophilic than PCL.

Table 6 Properties of the PCL-*b*-(PαN₃CL-*g*-PBA) films

Copolymers	Water contact angle	Water uptake (%)
PCL29-*b*-(PαN₃CL28-*g*-PBA21)	61	45.8
PCL29-*b*-(PαN₃CL6-*g*-PBA5)	65	25.4
PCL60-*b*-(PαN₃CL34-*g*-PBA17)	70	5.94

Table 5 Effect of the concentration on the size of micelle

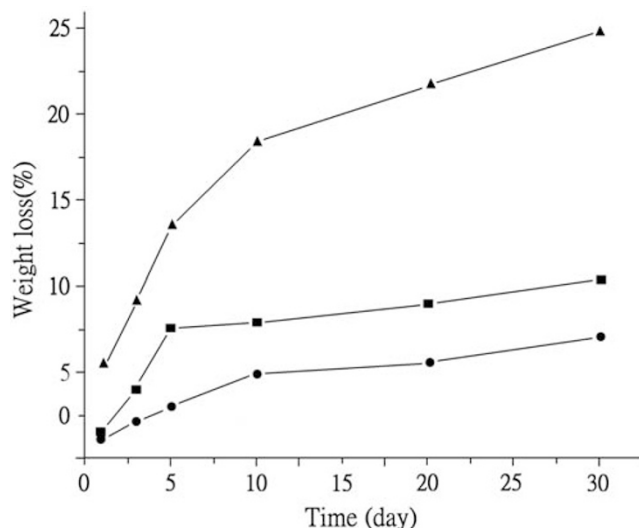| Micelle concentration (mg l⁻¹)	Size (nm)	
	PCL29-b-(PαN₃CL6-g-PBA5)	PCL29-b-(PαN₃CL28-g-PBA21)
300	176.9 ± 43.1	94.3 ± 28.6
150	176.5 ± 44.4	94.5 ± 30.3
75	177.7 ± 50.7	98.1 ± 12.6
37.5	179.9 ± 69.9	99.8 ± 32.5
4.69	188.7 ± 59.6	105.6 ± 35.7
2.93	192.6 ± 44.6	113.4 ± 63.4

Figure 7 Weight loss of block-graft copolymers (▲) PCL29-*b*-(PαN₃CL6-*g*-PBA5), (■) PCL29-*b*-(PαN₃CL28-*g*-PBA21), (●) PCL60-*b*-(PαN₃CL34-*g*-PBA17) treated in 0.067 M PBS (pH 7.4) at 37 °C.

Preliminary *in vitro* degradable study

As a biodegradable model, the *in vitro* degradation of block-graft PCL-*b*-(PαN₃CL-g-PBA) was evaluated from the weight loss of the sample in a thin film at 37 °C under physiological conditions (pH 7.4). Figure 7 depicts the results. After immersion for 30 days, the weight losses of the copolymers were 25.6 wt% for PCL30-*b*-(PαN₃CL6-g-PBA5), 9.9 wt% for PCL30-*b*-(PαN₃CL28-g-PBA21) and 7.2 wt% for PCL60-*b*-(PαN₃CL34-g-PBA17). Increasing the molecular weight and the length of the hydrophobic segment in the copolymers decreased their hydrophilicity, thus resulting in lower molecular weight losses.

Conclusions

This research studied a click strategy for modifying the hydrophilic–hydrophobic balance of polymers and successfully prepared novel block-graft amphiphilic copolymers consisting of a hydrophilic segment (PαN₃CL-g-PBA) and a hydrophobic segment (PCL). This work performed structural analyses including ^{1}H NMR and FT-IR to confirm the conjugation of these polymers. Thermal analysis reveals that PCL-*b*-(PαN₃CL-*g*-PBA) copolymers have lower melting points than do their corresponding homopolymers. Varying the amount of PαN₃CL-*g*-PBA or PCL in copolymers changes their hydrophilic abilities. The average micelle size is around 90–190 nm, and can be changed by varying the block-graft copolymer composition. These copolymers degrade under physiological conditions.

1 Kataoka, K., Harada, A. & Nagasaki, Y. Block copolymer micelles for drug delivery: design, characterization and biological significance. *Adv. Drug Deliv. Rev.* **47,** 113–131 (2001).
2 Lavasanifar, A., Samuel, J. & Kwon, G. S. Poly(ethylene oxide)-block-poly(l-amino acid) micelles for drug delivery. *Adv. Drug Deliv. Rev.* **54,** 169–190 (2002).
3 Liggins, R. T. & Burt, H. M. Polyether–polyester diblock copolymers for the preparation of paclitaxel loaded polymeric micelle formulations. *Adv. Drug Deliv. Rev.* **54,** 191–202 (2002).
4 Bae, Y., Fukushima, S., Harada, A. & Kataoka, K. Design of environment-sensitive supramolecular assemblies for intracellular drug delivery: polymeric micelles that are responsive to intracellular pH change. *Angew. Chem. Int. Ed.* **42,** 4640–4643 (2003).
5 Riess, G. Micellization of block copolymers. *Prog. Polym. Sci.* **28,** 1107–1170 (2003).
6 Discher, D. E. & Eisenberg, A. Polymer vesicles. *Science* **297,** 967–973 (2002).
7 Ivanova, R., Komenda, T., Bonné, T. B., Lüdtake, K., Mortensen, K., Pranzas, P. K., Jordan, R. & Papadakis, C. M. Micellar structures of hydrophilic/lipophilic and hydrophilic/fluorophilic poly(2-oxazoline) diblock copolymers in water. *Macromol. Chem. Phys.* **209,** 2248–2258 (2008).
8 Sundararaman, A., Stephan, T. & Grubbs, R. B. Reversible restructuring of aqueous block copolymer assemblies through stimulus-induced changes in amphiphilicity. *J. Am. Chem. Soc.* **130,** 12264–12265 (2008).
9 Chen, S., Zhang, X. Z., Cheng, S. X., Zhuo, R. X. & Gu, Z. W. Functionalized amphiphilic hyperbranched polymers for targeted drug delivery. *Biomacromolecules* **9,** 2578–2585 (2008).
10 O'Reilly, R. K., Joralemon, M. J., Hawker, C. J. & Wooley, K. L. Facile synthesis of surface-functionalized micelles and shell cross-linked nanoparticles. *J. Polym. Sci., Part A: Polym. Chem.* **44,** 5203–5217 (2006).
11 Zarafshani, Z., Akdemir, Ö. & Lutz, J. F. A click strategy for tuning *insitu* the hydrophilic-hydrophobic balance of AB macrosurfactants. *Macromol. Rapid Commun.* **29,** 1161–1166 (2008).
12 van Dongen, S. F. M., Nallani, M., Schoffelen, S., Cornelissen, J. J. L. M., Nolte, R. J. M. & van Hest, J. C. M A block copolymer for functionalisation of polymersome surfaces. *Macromol. Rapid Commun.* **29,** 321–325 (2008).
13 Binder, W. H. & Sachsenhofer, R. Click chemistry in polymer and materials science. *Macromol. Rapid Commun.* **28,** 15–54 (2007).
14 Kolb, H. C., Finn, M. G. & Sharpless, K. B. Click chemistry: diverse chemical function from a few good reactions. *Angew. Chem. Int. Ed.* **40,** 2005–2021 (2001).
15 Zhang, X., Lian, X., Liu, L., Zhang, J. & Zhao, H. Synthesis of comb copolymers with pendant chromophore groups based on RAFT polymerization and click chemistry and formation of electron donor-acceptor supramolecules. *Macromolecules* **41,** 7863–7869 (2008).
16 Malkoch, M., Thibault, R. J., Drockenmuller, E., Messerschmidt, M., Voit, B., Russell, T. P. & Hawker, C. J. Orthogonal approaches to the simultaneous and cascade functionalization of macromolecules using click chemistry. *J. Am. Chem. Soc.* **127,** 14942–14949 (2005).
17 Bouillon, C., Meyer, A., Vidal, S., Jochum, A., Chevolot, Y., Cloarec, J. P., Praly, J. P., Vasseur, J. J. & Morvan, F. Microwave assisted click chemistry for the synthesis of multiple labeled-carbohydrate oligonucleotide on solid support. *J. Org. Chem.* **71,** 4700–4702 (2006).
18 Ranjan, R. & Brittain, W. J. Tandem RAFT polymerization and click chemistry: an efficient approach to surface modification. *Macromol. Rapid Commun.* **28,** 2084–2089 (2007).
19 Jiang, X., Vogel, E. B., Smith, M. R. III & Baker, G. L. Clickable polyglycolides: tunable synthons for thermoresponsive, degradable polymers. *Macromolecules* **41,** 1937–1944 (2008).
20 Gondi, S. R., Vogt, A. P. & Sumerlin, B. S. Versatile pathway to functional telechelics via RAFT polymerization and click chemistry. *Macromolecules* **40,** 474–481 (2007).
21 Sumerlin, B. S., Tsarevsky, V., Louche, G., Lee, R. Y. & Matyjaszewski, K. Highly efficient click functionalization of poly(3-azidopropyl methacrylate) prepared by ATRP. *Macromloecules* **38,** 7540–7545 (2005).
22 Lee, R. S. & Huang, Y. T. Synthesis and characterization of amphiphilic block-graft MPEG-*b*-(PαN₃Cl-*g*-alkyne) degradable copolymers by ring-opining polymerization and click chemistry. *J. Polym. Sci. Part A: Polym. Chem.* **46,** 4320–4331 (2008).
23 Lenior, S., Riva, R., Lou, X., Detrembleur, Ch., Jérôme, R. & Lecomte, Ph. Ring-opening polymerization of α-chloro-ε-caprolactone and chemical modification of poly(α-chloroε-caprolactone) by atom transfer radical processes. *Macromolecules* **37,** 4055–4061 (2004).
24 Wilhelm, M., Zhao, C. L., Wang, Y., Xu, R., Winnik, M. A., Mura, J. L., Riess, G. & Croucher, M. D. Poly(styrene-ethylene oxide) block copolymer micelle formation in water: a fluorescence probe study. *Macromolecules* **24,** 1033–1040 (1991).
25 Provencher, S. W. & Hendrix, J. Direct determination of molecular weight distributions of polystyrene in cyclohexane with photon correlation spectroscopy. *J. Chem. Phys.* **69,** 4273–4276 (1978).
26 Chiu, F. C., Lai, C. S. & Lee, R. S. Synthesis functional poly(carbonate-*b*-ester) copolymers and micellar characterizations. *J. Appl. Polym. Sci.* **106,** 283–292 (2007).
27 Riva, R., Schmeits, S., Jérôme, C., Jérôme, R. & Lecomte, Ph. Combination of ring-opening polymerization and 'click chemistry': toward functionalization and grafting of poly(ε-caprolactone). *Macromolecules* **40,** 796–803 (2007).
28 Parrish, B., Breitenkamp, R. B. & Emrick, T. PEG- and peptide-grafted aliphatic polyesters by click chemistry. *J. Am. Chem. Soc.* **127,** 7404–7410 (2005).
29 Allen, C., Maysinger, D. & Eisenberg, A. Nano-engineering block copolymer aggregates for drug delivery. *Colloids and Surfaces B* **16,** 3–27 (1999).
30 Wu, J., Pearce, E. M., Kwei, T. K., Lefebvre, A. A. & Balsara, N. P. Micelle formation of a rod–coil diblock copolymer in a solvent selective for the rod block. *Macromolecules* **35,** 1791–1796 (2002).